XVIII Physics in Collision
Frascati, June 18th-19th, 1998
Conference Proceedings, pp. 000-000

A SUMMARY OF RECENT COLOR COHERENCE RESULTS

Nikos Varelas
Department of Physics, University of Illinois at Chicago, Chicago, Illinois 60607, USA

ABSTRACT

Recent experimental results on color coherence phenomena from e^+e^-, ep, and $p\overline{p}$ collisions are presented. The data are compared to analytic perturbative QCD calculations based on the modified leading logarithm approximation and the local parton hadron duality hypothesis.

1 Introduction

An important goal in the study of high energy hard collision properties is the detailed understanding of the hadronic final state and its characteristic jet structure. Perturbative QCD (pQCD) calculations have been used to describe the production of jet final states. However, the jet structure still relies on phenomenological models to describe how the partonic cascade evolves into the final state of hadrons.

In the picture implemented in Monte Carlo (MC) simulations, it is assumed that first the primarily produced partons from the hard scatter evolve via softer gluon and quark emission according to pQCD into jets of partons. This process continues until a cut-off k_T scale ($Q_0 \sim 1$ GeV) is reached as pQCD calculations are valid for $Q_0 >> \Lambda_{QCD}$. After this phase, non-perturbative processes take over which "cluster" the final partons into color singlet hadronic states via a mechanism described by phenomenological fragmentation models, like the Lund "string" [1] or the "cluster" [2] fragmentation model. These models usually involve quite a number of *a priori* unknown parameters that need to be tuned to the data.

A different and purely analytical approach giving quantitative predictions of hadronic spectra is based on the concept of "Local Parton Hadron Duality" (LPHD) [3]. The key assumption of this hypothesis is that the particle yield is described by a parton cascade where the conversion of partons into hadrons occurs at a low virtuality scale, of the order of hadronic masses ($Q_0 \sim 200$ MeV), independent of the scale of the primary hard process, and involves only low-momentum transfers; it is assumed that the results obtained for partons apply to hadrons as well. This correspondence of the partonic properties to the hadronic ones should only be considered in an inclusive and average sense.

LPHD may be connected to pre-confinement properties of QCD which ensure that color charges are compensated locally [4]. According to the preconfinement idea, color singlet clusters are formed during that phase. These clusters evolve into hadronic clusters via a smooth transformation such that local properties remain conserved in an average sense. With LPHD, only two essential parameters are involved in the perturbative description: the effective QCD scale Λ and a (transverse momentum) cut-off parameter Q_0, resulting in a highly constrained theoretical framework; non-perturbative effects are essentially reduced to normalization constants. Within the LPHD approach, pQCD calculations have been carried out in the simplest case (high energy limit) in the Double Log Approximation (DLA) [5, 6], or in the Modified Leading Log Approximation (MLLA) [3, 7, 8], which includes higher order terms of relative order $\sqrt{\alpha_s}$ (e.g., finite energy corrections) that are essential for quantitative agreement with data at present energies.

2 Color Coherence

Coherence phenomenon is an intrinsic property of QCD (and in fact of any gauge theory). Its observation is important in the study of strong interactions and in the search for deviations from the Standard Model.

Color coherence phenomena in the final state have been very well established from early '80's in e^+e^- annihilations [9, 10, 11, 12, 13, 14], in what has been termed the "string" [15] or "drag" [16] effect. Particle production in the region between the quark and antiquark jets in $e^+e^- \to q\bar{q}g$ events is suppressed. In pQCD such effects arise from interference between the soft gluons radiated from the q, $\bar{q}$, and g. While quantum mechanical interference effects are expected in QCD, it is important to investigate whether such effects survive the non-perturbative hadronization process, for a variety of reactions over a broad kinematic range, as predicted by LPHD.

It is instructive to separate the color coherence phenomena into two regions: the int<u>ra</u>jet and int<u>er</u>jet coherence [17, 18]. The intrajet coherence deals with the coherent effects in partonic cascades, resulting on the average, in the angular ordering (AO) of the sequential parton branches which give rise to the *hump-backed* shape of particle spectra inside QCD jets. The interjet coherence is responsible for the string/drag effect and deals with the angular structure of soft particle flows when three or more energetic partons are involved in the hard process.

The AO approximation is an important consequence of color coherence. It results in the suppression of soft gluon radiation in the partonic cascade in certain regions of phase space. For the case of outgoing partons, AO requires that the emission angles of soft gluons decrease monotonically as the partonic cascade evolves away from the hard process. The radiation is confined to a cone centered on the direction of one parton, and is bounded by the direction of its color–connected partner. Outside this region the interference of different emission diagrams becomes destructive and the azimuthally integrated amplitude vanishes to leading order. MC simulations including coherence effects probabilistically by means of AO are available for both initial and final state evolutions.[1] Another way to incorporate coherence effects in parton shower event generators is by using the color dipole cascade model, implemented in the ARIADNE [19] MC program.

The AO is an important element of the DLA and MLLA analytic pQCD calculations, which provides the probabilistic interpretation of soft-gluon cascades. In fact beyond the MLLA a probabilistic picture of the parton cascade evolution is not feasible due to $1/N_c^2$ (where N_c is the number of colors) suppressed soft interference contributions that appear in the higher-order calculations [7, 18].

In this report we present current experimental results on observables that test the LPHD hypothesis in the context of color coherence phenomena from e^+e^-, ep, and $p\overline{p}$ collisions.

3 Intrajet Coherence Results

The study of multiparticle production in hard collision processes can yield valuable information about the characteristic features of the partonic branching processes in QCD and the transition from colored partons to colorless hadrons. It is of great importance to know whether a smooth transition exists between a purely perturbative regime and the soft momentum region. Recent results on particle production are discussed in this section.

3.1 Hump-Backed Plateau

A striking prediction of the perturbative approach to QCD jet physics is the depletion of soft particle production and the resulting approximately Gaussian shape of the inclusive distribution in the variable $\xi = \log(E_{jet}/p) = \log(1/x_p)$ for particles with momentum p in a jet of energy E_{jet}—the famous "hump-back plateau" (see Ref. [18] and earlier references therein). Due to the *intrajet* coherence of gluon radiation (resulting on

[1]Parton shower event generators incorporate AO effects in the initial state as the time reverse process of the outgoing partonic cascade, i.e., the emission angles increase for the incoming partons as the process develops from the initial hadrons to the hard subprocess.

the average in the AO of sequential branching), not the softest partons but those with intermediate energies ($E_h \propto E_{jet}^{0.3-0.4}$) multiply most effectively in QCD cascades.

According to the expectations of the MLLA+LPHD the inclusive momentum spectra of hadrons produced is given by:

$$\frac{1}{\sigma}\frac{d\sigma}{d\xi} = Const \cdot f_{MLLA}(\xi, Y, \lambda) \tag{1}$$

where

$$Y = \log\frac{E_{jet}}{Q_0}; \lambda = \log\frac{Q_0}{\Lambda} \tag{2}$$

The function f_{MLLA} is the MLLA formula for the number of final state partons per unit ξ per event and is approximately Gaussian in ξ. To check the validity of the MLLA+LPHD approach, it is interesting to study the energy evolution of the maximum, ξ^*, of the ξ distribution. The prediction of the dependency of ξ^* on the center of mass energy can be expressed as (see Ref. [17] and earlier references therein):

$$\xi^* = Y(1/2 + \sqrt{C/Y} - C/Y) + F_h(\lambda) \tag{3}$$

where

$$C = \left(\frac{11N_c/3 + 2n_f/3N_c^2)}{4N_c}\right)^2 \cdot \frac{N_c}{11N_c/3 - 2n_f/3} \tag{4}$$

with n_f the number of quark flavors and $F_h(\lambda)$ a function that depends on the hadron type, h, through the ratio λ:

$$F_h(\lambda) = -1.46\lambda + 0.207\lambda^2 \pm 0.06 \tag{5}$$

The shapes of the measured particle energy spectra in e^+e^- annihilation from early '90's have been surprisingly close, over the whole momentum range down to momenta of a few hundred MeV, to the MLLA+LPHD predictions. These observations can be taken as evidence that the perturbative phase of the cascade development indeed leaves its imprint on the final state hadrons supporting the hypothesis that color coherence effects survive the hadronization process as suggested by LPHD.

Recently, new data on charged particle spectra, exploring higher energy regimes, have become available from LEP, HERA, and TEVATRON. The HERA experiments concentrate on the "current" fragmentation region in DIS (fragmentation products of the outgoing quark) and perform the analysis in the Breit frame, where the exchanged boson is completely spacelike. The DIS current fragmentation functions at a momentum transfer Q are analogous to the e^+e^- fragmentation functions at center of mass energy equal to Q [20]. The new data confirm with much increased statistical significance the features observed in e^+e^-: approximately Gaussian shape of the ξ spectra with peak-position and width increasing with Q as predicted in MLLA.

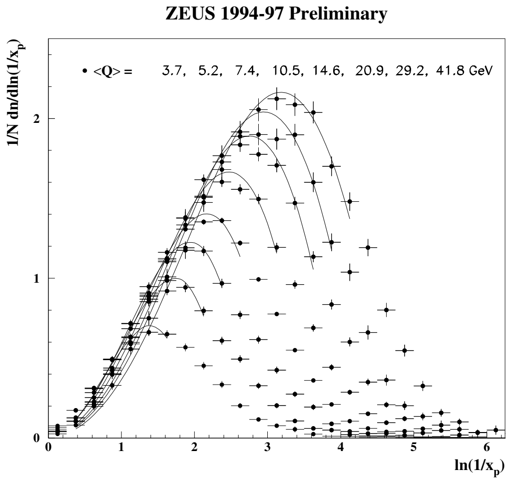

(a) Evolution of the $1/Ndn/d\log(1/x_p)$ distributions with Q. The curves are MLLA fits.

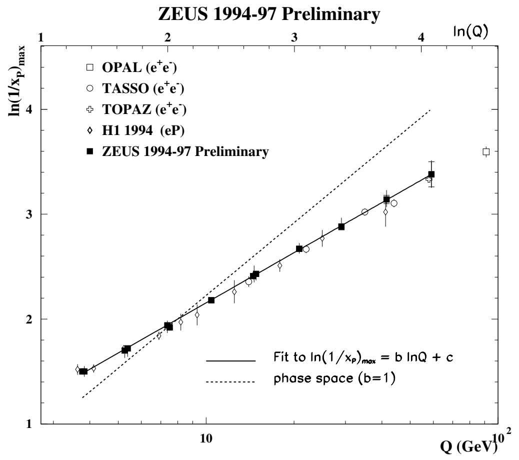

(b) Evolution of the peak position $log(1/x_p)_{max}$ with Q.

Figure 1: Comparison of preliminary ZEUS inclusive charged particle momentum distributions with MLLA predictions and e^+e^- data.

Figure 1a shows preliminary ξ distributions for charged particles in the current fragmentation region of the Breit frame as a function of Q from ZEUS. These distributions are approximately Gaussian in shape with mean charged multiplicity given by the integral of the distributions. As Q increases the multiplicity increases and the peak of the distribution shifts to larger values of ξ (i.e., smaller values of momenta). Figure 1b shows this peak position, $\log(1/x_p)_{max}$, as a function of Q for the ZEUS data and of $\sqrt{s}$ for the e^+e^- data. Over the range shown the peak moves from ≈ 1.5 to 3.3. The ZEUS data points are consistent with those from TASSO and TOPAZ and a clear agreement in the rate of growth of the ZEUS points with the OPAL data at higher Q is observed. From Fig. 1b it is clear that the ZEUS data are incompatible with the assumption of an incoherent branching picture or a simple phase-space model ($\xi^* \approx Y + const$). ZEUS also fitted the MLLA predictions (eq. 3) to their ξ^* evolution data, assuming $Q_0 = \Lambda \equiv Q_{eff} \equiv \Lambda_{eff}$, and extracted a value of $\Lambda_{eff} \approx 245$ MeV which is in agreement with a similar value obtained from H1, CDF, or combined e^+e^- data. Notice that decreasing Q_0 means extending the responsibility of the perturbative stage beyond its formal range of applicability. However, in MLLA calculations this limit is smooth yielding a finite result even if the coupling gets arbitrarily large.

Figures 2 and 3 show similar distributions from the H1 and L3 experiments. A simultaneous MLLA fit to the peak and width values obtained from the present H1 data alone yields a value of $\Lambda_{eff} = 0.21 \pm 0.02$ GeV [21]. From Fig. 3b we see that the DLA calculations clearly disagree with the e^+e^- data. The finite energy corrections included in the MLLA predictions seem important. We also notice that the value of ξ^* at the Z^0 corresponds to the rather low momenta $x_p \approx 0.02$ or $p \approx 1$ GeV (Fig. 3a).

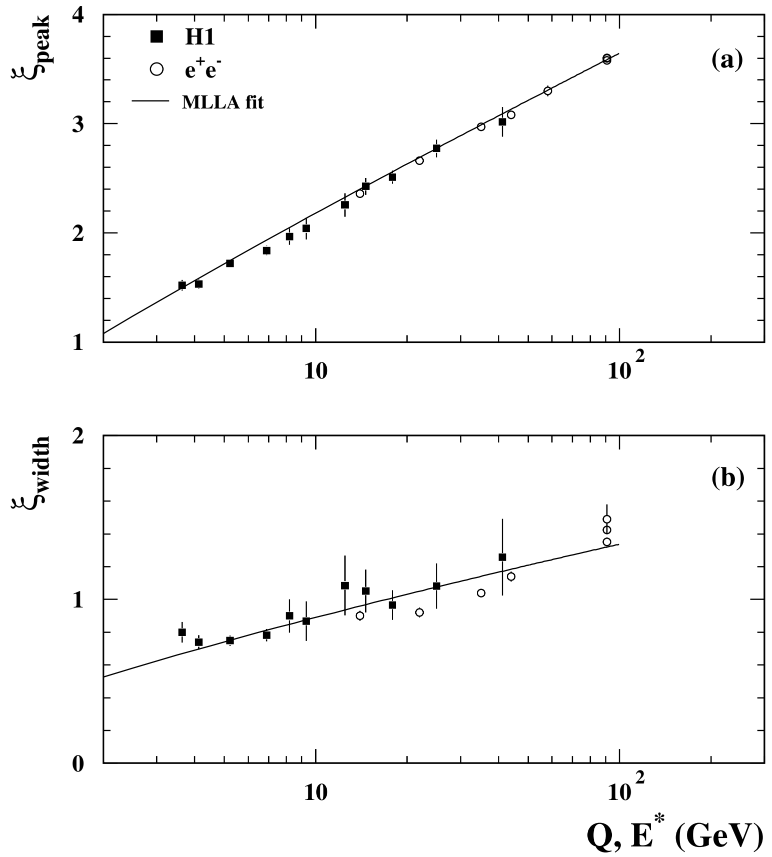

Figure 2: H1 results (solid symbols) showing the evolution of (a) the peak and (b) the width of the fragmentation function as a function of Q compared to e^+e^- results (open symbols) as a function of the center of mass energy, E^*. The solid line is a fit to MLLA expectations.

Confirmation of the MLLA+LPHD approach has also been presented by CDF. This experiment studies charged particle momentum distributions in subsamples of dijet events. For fixed dijet masses in the range $83 < M_{\rm JJ} < 625$ GeV/c^2, the ξ distribution of tracks, within cones of various opening angle Θ (with respect to the jet axis), is studied (see Fig. 4a). As dijet mass $\times$ jet opening angle increases, the peak of the spectrum, ξ_o, shifts towards larger values of ξ in perfect agreement with the e^+e^- data, as shown in Fig. 4b. The MLLA fit (superimposed in Fig. 4b) is in excellent agreement with the data and yields $Q_{eff} = 234 \pm 2(stat) \pm 15(syst)$ MeV, confirming that in this approximation the domain of pQCD extends down to $Q_{eff} \sim \Lambda_{QCD}$. Similar analyses should be possible in DIS and photoproduction at HERA but have not yet been attempted.

3.2 Identified Particle Spectra

The ξ-spectra for a variety of identified particles/resonances has been studied at the Z^0 pole at SLAC and at LEP. Recently the SLD Collaboration has reported measurements of the differential production cross sections as a function of x_p of several identified hadron and antihadron species in inclusive hadronic Z^0 decays, as well as separately for

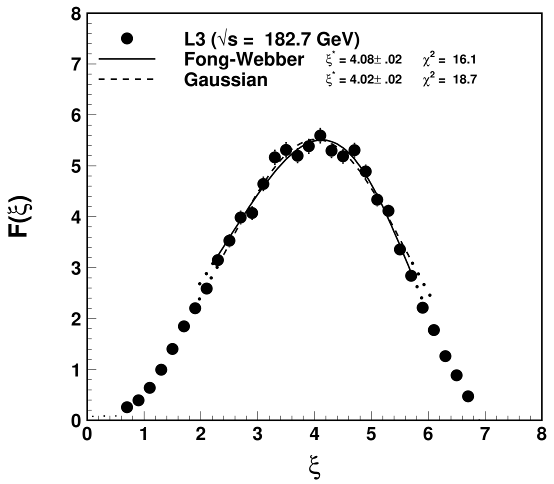

(a) $1/Ndn/dlog(1/x_p)$ distribution at 183 GeV. The curves are MLLA fits with different Gaussian parametrizations.

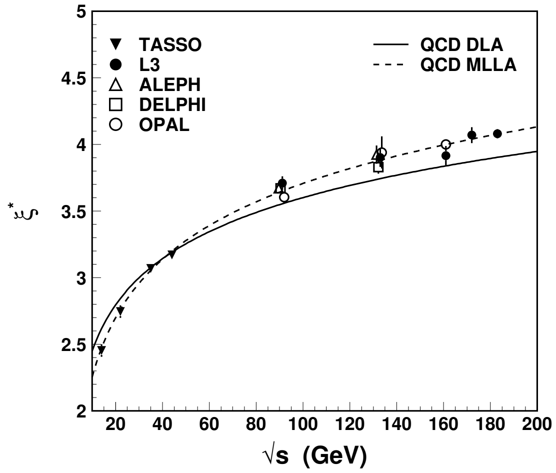

(b) Evolution of the peak position ξ^* with energy. The dashed line is a MLLA fit and the solid line is a fit to DLA. Clearly DLA disagrees with the data.

Figure 3: Comparison of preliminary L3 inclusive charged particle momentum distributions with MLLA predictions

Z^0 decays into light (u, d, s), c, and b flavors [22]. These results have been compared to MLLA as well as the predictions of three fragmentation models.

The fitted peak positions ξ^* for the various particles are plotted as a function of the hadron mass in Fig. 5, along with averages of similar measurements from experiments at LEP [23], with which they are consistent. The distribution for pions peaks at a higher ξ value than those of the other hadron species, but otherwise there is no obvious mass-dependence.[2] We notice that within the framework of the MLLA+LPHD picture there is no recipe for relating the Q_0 cut-off parameter to the masses of the produced hadrons and their quantum numbers.

The DELPHI Collaboration has recently reported preliminary results on the production of charged and neutral kaons, protons, and Λs at center of mass energies above the Z^0 pole. [24]. The data are found to be in good agreement with the MLLA predictions. This comparison confirms the perturbative expectation (eq. 3) that for different particle species the energy dependence of ξ^* is universal. The fit of the data points to expression (3), where $F_h(Q_0)$ was taken as a free parameter and Λ was fixed to 150 MeV (this value comes from the description of the pion spectra with $\Lambda = Q_0$) yielded a value for Q_0 of about 330 MeV consistent for the different particle types.

[2]One may also argue that Fig. 5 indicates that the peak position ξ^* decreases as a function of mass differently for baryons and mesons. These results may provide additional insights concerning the LPHD concept.

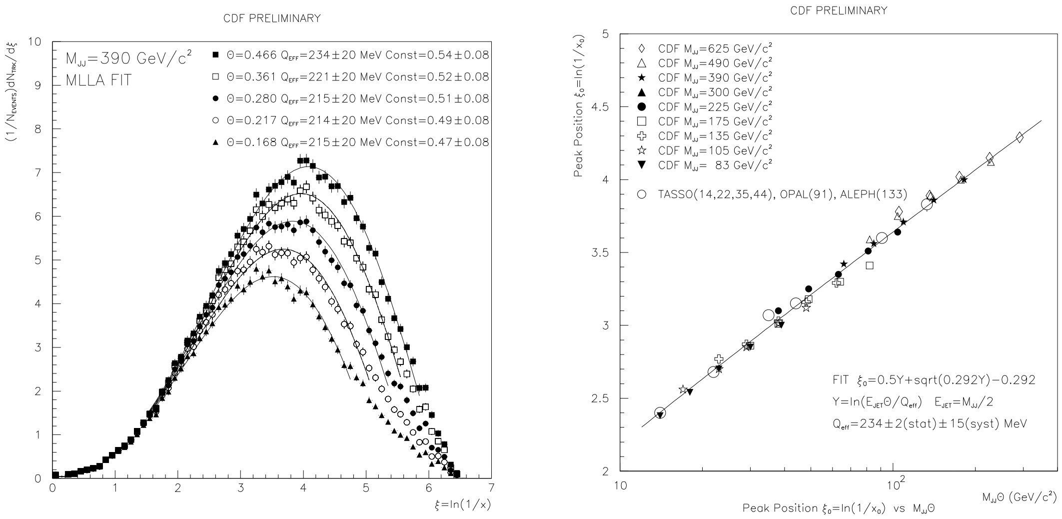

(a) Evolution of ξ with jet opening angle, Θ, for $M_{\rm JJ} = 390$ GeV.

(b) Evolution of the peak position with $M_{\rm JJ}\Theta$.

Figure 4: Comparison of preliminary CDF inclusive momentum distributions with MLLA predictions and e^+e^- annihilation data.

3.3 Invariant Energy Spectrum

The analytical perturbative approach allows one to predict the limit of the one-particle invariant density in QCD jets $Edn/d^3p \equiv dn/dy\, d^2\mathbf{p_T}$ at very small momenta p or, equivalently, in the limit of vanishing rapidity and transverse momentum [17]. If the dual description of hadronic and partonic states is adequate down to very small momenta, a finite, energy-independent limit of the invariant hadronic density, I_0, is expected. This is a direct consequence of the color coherence in soft gluon branching. Indeed, long wavelength gluons are emitted by the total conserved color current, which is independent of the internal structure of a jet and its energy. A possible rise of I_0 with center-of-mass energy would indicate that either coherence or the LPHD (or both) break down. Since color coherence is a general property of QCD as a gauge theory, it is the LPHD concept that is tested in measurements of the soft hadrons.

The e^+e^- annihilation data on charged and identified particle inclusive spectra have been found to follow the MLLA prediction surprisingly well, also at low center-of-mass energies. The invariant spectra at low momentum scale approximately (within 10%) between 1.6 and 161 GeV and agree with perturbative calculations which become very sensitive to the strong running of α_S at small scales [25].

The H1 Collaboration has reported the first Breit frame measurements of the invariant energy spectra in DIS as a function of Q [21]. For sufficiently high Q, the data show that the low-momentum limit in that region of phase space is essentially independent

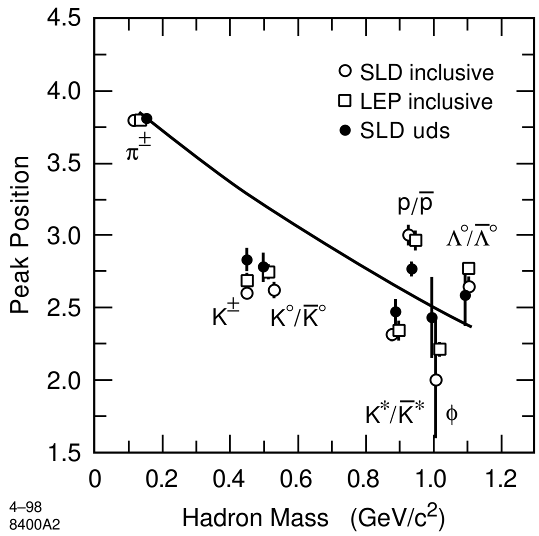

Figure 5: Peak positions ξ^* from fits to the ξ distributions in flavor-inclusive and light-flavor hadronic Z^0 decays. Also shown are the averages of similar flavor-inclusive results from experiments at LEP. The line is the result of an ad hoc exponential fit to the SLD light-flavor data.

of Q and indeed similar to that in e^+e^- annihilation.

4 Interjet Coherence Results in $p\overline{p}$ Interactions

The study of coherence effects in hadron–hadron collisions is considerably more subtle than that in e^+e^- annihilations due to the presence of colored constituents in both the initial and final states. During a hard interaction, color is transferred from one parton to another and the color–connected partons act as color antennae, with interference effects taking place in the initial or final states, or between the initial and final states. Gluon radiation from the incoming and outgoing partons forms jets of hadrons around the direction of these colored emitters. The soft gluon radiation pattern accompanying any hard partonic system can be represented, to leading order in $1/N_c$ as a sum of contributions corresponding to the color–connected partons. Within the perturbative calculations, this is a direct consequence of interferences between the radiation of various color emitters, resulting in the QCD coherence effects [16, 18, 26].

4.1 Multijets

Both the CDF [27] and DØ [28] Collaborations have measured spatial correlations between the softer third jet and the second leading-E_T jet in $p\overline{p} \rightarrow 3jets + X$ events to explore the initial-to-final state coherence effects in $p\overline{p}$ interactions.

In the DØ analysis the jets were reconstructed using a fixed-cone clustering algorithm with 0.5 cone radius. The corrected transverse energy of the highest-E_T jet of the event was required to be above 115 GeV while the third jet was required to have $E_T > 15$ GeV. The interference between the second and the third jet is displayed using the polar variables $R = \sqrt{(\Delta\eta)^2 + (\Delta\phi)^2}$ and $\beta = \tan^{-1}(\frac{sign(\eta_2)\cdot\Delta\phi}{\Delta\eta})$; where $\Delta\eta = \eta_3 - \eta_2$ and $\Delta\phi = \phi_3 - \phi_2$, in a search disk of $0.6 < R < \frac{\pi}{2}$. (Pseudorapidity $\eta = -\ln[\tan(\theta/2)]$, where θ is the polar angle of the jet with respect to the proton beam.)

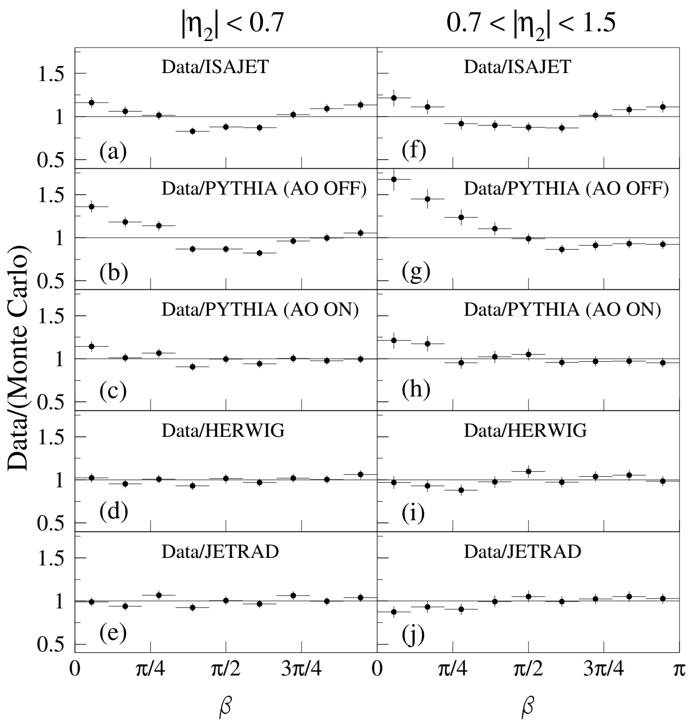

Figure 6: Ratio of β distributions between data and the predictions of: (a) ISAJET, (b) PYTHIA with AO off, (c) PYTHIA with AO on, (d) HERWIG, (e) JETRAD for the central region; and (f)-(j) for the forward region respectively. The error bars include statistical and uncorrelated systematic uncertainties.

Figure 6 shows the ratio of the β distributions for the DØ data relative to several MC predictions for both central ($|\eta_2| < 0.7$) and forward ($0.7 < |\eta_2| < 1.5$) regions. Detector position and energy resolution effects have been included in the MC simulations. The absence of color interference effects in ISAJET [29] results in a disagreement with the DØ β distributions. The data show a clear enhancement of events compared to ISAJET near the event plane (i.e., the plane defined by the directions of the second jet and the beam axis, $\beta = 0, \pi$) and a depletion in the transverse plane ($\beta = \frac{\pi}{2}$). This is consistent with the expectation from initial–to–final state color interference that the rate of soft jet emission around the event plane be enhanced with respect to the transverse plane. However, HERWIG 5.8 [2] which contains initial and final state interference effects implemented by means of the AO approximation of the parton cascade, agrees well with the data. The DØ data have also been compared to PYTHIA 5.7 [30] which also simulates the color interference effects with the AO approximation. The PYTHIA predictions include string fragmentation. Without AO the PYTHIA distributions are significantly different from the data, while with AO turned on there is much better agreement, although there are still some residual differences in the "near beam" region. Finally, the $\mathcal{O}(a_s^3)$ tree-level QCD prediction from JETRAD [31] describes the coherence effects seen in the data in both η regions.

4.2 W+Jets

In $p\overline{p} \rightarrow W + Jets$ events, the angular distribution of soft gluons about the colorless W boson is expected to be uniform, while the distribution around the jet is expected to have structure due to the colored partons in the jet. DØ studies these effects by comparing the distributions of soft particles around the W boson and opposing jet directions. This comparison reduces the sensitivity to global detector and underlying event biases that may be present in the vicinity of the W boson and the jet.

Once the W boson direction has been determined in the DØ detector, the opposing jet is identified by selecting the leading–E_T jet in the ϕ hemisphere opposite to the W boson. Annular regions are drawn around both the W boson and the jet in (η, ϕ) space. The angular distributions of towers ($\Delta\eta \times \Delta\phi = 0.1 \times 0.1$) above the 250 MeV threshold are measured in these annular regions using the polar variables $R = \sqrt{(\Delta\eta)^2 + (\Delta\phi)^2}$ and $\beta_{W,Jet} = \tan^{-1}(\frac{sign(\eta_{W,Jet}) \cdot \Delta\phi_{W,Jet}}{\Delta\eta_{W,Jet}})$; where $\Delta\eta_{W,Jet} = \eta_{Tower} - \eta_{W,Jet}$ and $\Delta\phi_{W,Jet} = \phi_{Tower} - \phi_{W,Jet}$, in a search disk of $0.7 < R < 1.5$. Color coherence effects are expected to manifest themselves as an enhancement in the energetic tower distribution around the tagged jet in the event plane relative to the transverse plane (when compared with the W boson distribution). These coherence effects are similar to the string/drag effects observed in the $e^+e^- \rightarrow q\overline{q}g$ events.

DØ has analyzed $W \rightarrow e + \nu$ events requiring at least one jet with $E_T > 10$ GeV, $|\eta_{Jet}| < 0.7$, and W boson rapidity $|y_W| < 0.7$. Additionally, the z component of the event vertex was restricted to $|z_{vtx}| < 20$ cm to retain the projective nature of the calorimeter towers.

The data angular distributions are compared to three MC samples, generated with different levels of color coherence effects, using the PYTHIA 5.7 parton shower event generator and passed through a full detector simulation. PYTHIA, with both AO and string fragmentation (SF) implemented, accounts for color coherence effects at both the perturbative and non-perturbative levels. Turning off AO removes the perturbative contribution, and using independent fragmentation (IF) eliminates the non-perturbative component. Finally, a comparison to a MLLA+LPHD pQCD calculation of Khoze and Stirling [32] is also presented.

Figure 7a shows the ratio of the tower multiplicity around the jet to the tower multiplicity around the W as a function of β. The number of towers is greater for the jet than for the W boson and the excess is enhanced in the event plane ($\beta = 0, \pi$) and minimized in the transverse plane ($\beta = \frac{\pi}{2}$), consistent with the expectation from initial–

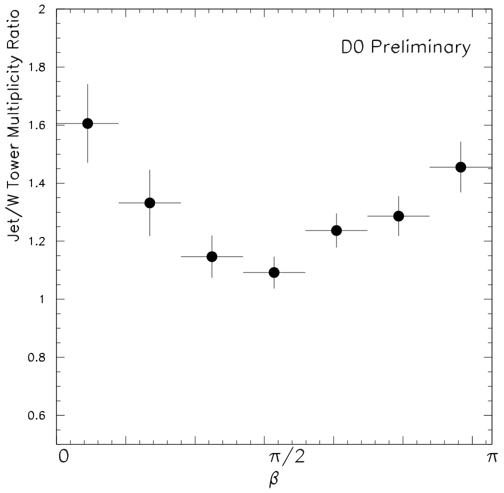

(a) Jet/W tower multiplicity ratio as a function of β.

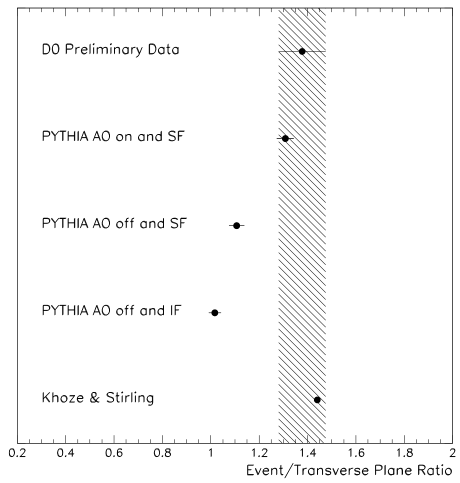

(b) Ratio of event plane to transverse plane of Jet/W tower multiplicity for DØ data, PYTHIA with various coherence implementations, and a MLLA QCD calculation. The errors are statistical only.

Figure 7: DØ preliminary results on $W+$ Jets coherence.

to–final state color interference effects. The errors include only statistical uncertainties, which are significantly larger than all systematic uncertainties considered.

A measure of the observed color coherence effect is obtained by calculating the Jet/W tower multiplicity enhancement of the event plane ($\beta = 0, \pi$) to the transverse plane ($\beta = \pi/2$), which would be expected to be unity in the absence of color coherence effects. This ratio of ratios is insensitive to the overall normalization of the individual distributions, and MC studies have shown that it is relatively insensitive to detector effects. Figure 7b compares the data to the various PYTHIA predictions and to the MLLA+LPHD calculation. There is good agreement with PYTHIA with AO on and string fragmentation, and disagreement with AO off and string fragmentation or AO off and independent fragmentation. These comparisons imply that for the process under study, string fragmentation alone cannot accommodate the effects seen in the data. The AO approximation is an element of parton-shower event generators that needs to be included if color coherence effects are to be modeled successfully. Finally, the analytic predictions by Khoze and Stirling are in agreement with the data, giving additional evidence supporting the validity of the LPHD hypothesis.

5 A Color "Reconnection" Study in Hadronic Z^0 Decays

Most implementations of QCD coherence effects are based on a probabilistic scheme (e.g., AO approximation) where interference terms of relative order $1/N_c^2$ are ignored (the so-called large N_c approximation). In this picture the way the partons are connected to form color singlet states is uniquely specified. For example, in $Z^0 \rightarrow q\bar{q}gg$ events, in which two gluons are radiated against a $q\bar{q}$ pair from a Z^0 decay, the quark is color-connected to one of the gluons, this gluon is connected to the second gluon, and the second gluon is connected to the antiquark. Thus, the entire event consists of a color singlet state.

Beyond the large N_c approximation, the color configurations that the partons follow when connected to each other is not longer specified uniquely. In our example, the possibility that the q and $\bar{q}$ form a color singlet by themselves, with the two gluons gg forming a separate color singlet, is suppressed by a factor of $1/(N_c^2-1)$ relative to the leading configuration described above. The possibility to connect the partons in this latter manner is often called color "reconnection" or recoupling. Color "reconnection" is, however, an unfortunate terminology since the partons have not been physically **re**-connected.

Color reconnection effects are of fundamental importance for our understanding of the confinement mechanism. Does Nature select a particular configuration at random or some configuration is dynamically favored in forming color singlet states? Recently there has been a lot of interest on color reconnection due to the possibility that higher order color rearrangement diagrams could affect the W mass measurement at LEP-II. So far there has not been any experimental evidence on this expectation suggesting that these effects might be small in WW pair events [33].

The OPAL Collaboration has performed a search for color reconnection effects in $Z^0 \rightarrow q\bar{q}g_{inc}$ events, in which the q and $\bar{q}$ are identified quark (and antiquark) jets which appear in the same hemisphere of an event. The object g_{inc}, taken to be the g jet, is defined by all particles observed in the hemisphere opposite to that containing the q and $\bar{q}$ jets. In the limit that the q and $\bar{q}$ are collinear the gluon jets are produced from a color singlet point source, corresponding to the definition of gluon jets in the theoretical calculations.

The ARIADNE MC program with and without reconnection effects is compared to the OPAL preliminary data. The version of ARIADNE with reconnection predicts fewer (more) particles at small (large) rapidities and energies than are observed in either the data or other standard MC programs. Furthermore, ARIADNE with reconnection predicts a smaller charged particle multiplicity for the g_{inc} hemisphere than the other standard MC simulations or the multiplicity measured in data (see Fig. 8). Figure 8 also shows the multiplicity distributions for light quark (u, d, s) jets in $Z^0 \rightarrow q\bar{q}$ decays, which appear to be insensitive to reconnection effects.

OPAL performed two quantitative tests to assess the difference between the data and the predictions of ARIADNE. The first test is based on the comparison of the ratio of the mean gluon to light quark jet charged particle multiplicity between the data and the various MC predictions, and the second one is based on the probability for a g_{inc} jet to

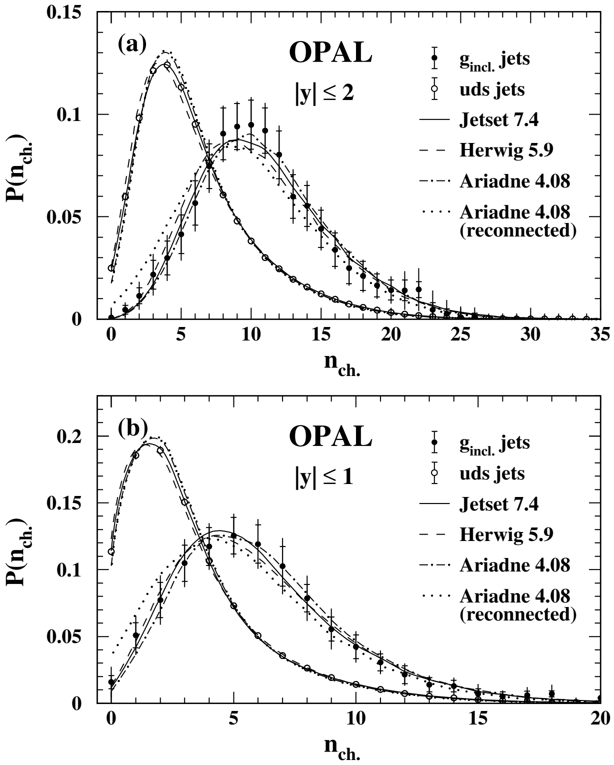

Figure 8: OPAL preliminary results on charged particle multiplicity in the rapidity intervals (a) $|y| \leq 2$ and (b) $|y| \leq 1$ for 41.6 GeV "g_{inc} jets" and 45.6 GeV uds quark jets. The total uncertainties are shown by vertical lines. The statistical uncertainties are indicated by horizontal bars. The predictions of various parton shower MC event generators are also shown.

have five or fewer charged particles with $|y| \leq 2$. Both tests showed that the ARIADNE reconnection model is disfavored by the data, whereas the standard QCD MC programs (HERWIG, JETSET, and ARIADNE without reconnection) reproduce the experimental results well.

6 Conclusions

The high precision data from HERA, LEP, SLD, and TEVATRON have provided a detailed testing ground for the strong interactions. Beautiful agreement of the data, from e^+e^-, ep, and $p\overline{p}$ collisions, with analytic pQCD calculations, based on MLLA and LPHD, has been seen in several inclusive observables sensitive to color coherence phenomena. Although the support of the LPHD from the current data is strong, it is important to continue investigating the limitations of this picture, since it is not clear *a priori* for which observables and in which kinematic regions it applies. Finally, the traditional parton shower event generators which incorporate color coherence effects at the perturbative and non-perturbative stages seem to describe well the interjet coherence phenomena observed in $p\overline{p}$ collisions.

7 Acknowledgements

I express my deep appreciation to Valery Khoze for numerous valuable discussions on this work. I would also like to thank Alessandro De Angelis, Phil Burrows, Tony Doyle, Martin Erdmann, Costas Foudas, Bill Gary, Rick Van Kooten, Andrey Korytov, Joachim Mnich, and David Muller who provided me with material for this review. Special thanks to Valery Khoze, Hugh Montgomery, and Gregory Snow for their comments on this manuscript.

References

1. B. Andersson, G. Gustafson, G. Ingelman, and T. Sjöstrand, Phys. Rep. **97**, 31 (1983).
2. G. Marchesini *et al.*, Computer Physics Commun. **67**, 465 (1992).
3. Ya.I. Azimov, Yu.L. Dokshitzer, V.A. Khoze, and S.I. Troyan, Zeit. Phys. **C27**, 65 (1985) and **C31**, 213 (1986).
4. D. Amati and G. Veneziano, Phys. Lett. **83B**, 87 (1979); A. Bassetto, M. Ciafaloni and G. Marchesini, Phys. Lett. **B83**, 207 (1979); G. Marchesini, L. Trentadue and G. Veneziano, Nucl. Phys. **B181**, 335 (1981).
5. Yu.L. Dokshitzer, V.S. Fadin, and V.A. Khoze, Phys. Lett. **B115**, 242 (1982); Zeit. Phys. **C15**, 325 (1982).
6. A. Bassetto, M. Ciafaloni, and G. Marchesini, Phys. Rep. **C100**, 201 (1983).
7. Yu.L. Dokshitzer and S.I. Troyan, in Proc. 19th Winter School of the LNPI, Vol. 1, p.144; Leningrad preprint LNPI-922 (1984).
8. A.H. Mueller, Nucl. Phys. **B213**, 85 (1983); Erratum quoted ibid. **B241**, 141 (1984).
9. JADE Collaboration, W. Bartel *et al.*, Phys. Lett. **B101**, 129 (1981); Zeit. Phys. **C21**, 37 (1983); Phys. Lett. **B134**, 275 (1984); Phys. Lett. **B157**, 340 (1985).
10. TPC/2γ Collaboration, H. Aihara *et al.*, Phys. Rev. Lett. **54**, 270 (1985); Zeit. Phys. **C28**, 31 (1985); Phys. Rev. Lett. **57**, 945 (1986).
11. TASSO Collaboration, M. Althoff *et al.*, Zeit. Phys. **C29**, 29 (1985).
12. MARK2 Collaboration, P.D. Sheldon *et al.*, Phys. Rev. Lett. **57**, 1398 (1986).
13. OPAL Collaboration, M.Z. Akrawy *et al.*, Phys. Lett. **B247**, 617 (1990); Phys. Lett. **B261**, 334 (1991); P.D. Acton *et al.*, Phys. Lett. **B287**, 401 (1992); Zeit. Phys. **C58**, 207 (1993).

14. L3 Collaboration, M. Acciarri *et al.*, Phys. Lett. **B353**, 145 (1995).

15. B. Andersson, G. Gustafson, and T. Sjöstrand, Phys. Lett. **B94**, 211 (1980).

16. Ya.I. Azimov, Yu.L. Dokshitzer, V.A. Khoze, and S.I. Troyan, Phys. Lett. **B165**, 147 (1985); Sov. Journ. Nucl. Phys. **43**, 95 (1986).

17. For a recent discussion of the phenomenological status and comparisons to data, see V.A. Khoze and W. Ochs, Int. J. Mod. Phys. **A12**, 2949 (1997).

18. Yu.L. Dokshitzer, V.A. Khoze, A.H. Mueller, and S.I. Troyan, "Basics of Perturbative QCD", Editions Frontières (1991).

19. L. Lönnblad, Comp. Phys. Comm. **71**, 15 (1992).

20. L.V. Gribov, Yu.L. Dokshitzer, V.A. Khoze, and S.I. Troyan, Phys. Lett. **B202**, 276 (1988); Sov. Phys. JETP, **68**, 1303 (1988).

21. H1 Collaboration, C.Adloff *et al.* , Nucl. Phys. **B504**, 3 (1997).

22. SLD Collaboration, K. Abe *et al.* , SLAC-PUB-7766; subm. to Phys. Rev. D.

23. A. Böhrer, Phys. Rep. **291**, 107 (1997).

24. *http://wwwinfo.cern.ch/˜deangeli/ident.ps*

25. S. Lupia and W. Ochs, Phys. Lett. **B365**, 339 (1996); V.A. Khoze, S. Lupia and W. Ochs, to appear in Euro Phys. Journ. C (hep-ph/9711392).

26. R.K. Ellis, G. Marchesini, and B.R. Webber, Nucl. Phys. **B286**, 643 (1987); Erratum Nucl. Phys. **B294**, 1180 (1987).

27. CDF Collaboration, F. Abe *et al.*, Phys. Rev. D **50**, 5562 (1994).

28. DØ Collaboration, B. Abbott *et al.*, Phys. Lett. **B414**, 419 (1997).

29. F.E. Paige and S.D. Protopopescu, BNL report No. 38034, 1986 (unpublished).

30. T. Sjöstrand, Computer Physics Commun. **82**, 74 (1994).

31. W.T. Giele, E.W.N. Glover, and D.A. Kosower, Nucl. Phys. **B403**, 633 (1993); Phys. Rev. Lett. **73**, 2019 (1994).

32. V.A. Khoze and J. Stirling, Zeit. Phys. **C76**, 59 (1997).

33. M. Pepe-Altarelli, these proceedings (and references therein).